EVERUN - Enabling Power Consumption Monitoring in Underwater Networking Platforms

Giannis Kazdaridis*, Stratos Keranidis†, Polychronis Symeonidis*, Paulo Sousa Dias‡,

Pedro Gonçalves‡, Bruno Loureiro‡, Petrika Gjanci§ and Chiara Petrioli§

*Department of Electrical and Computer Engineering, University of Thessaly, Greece

†Gridnet S.A., Volos, Greece

‡Underwater Systems and Technology Laboratory, Faculdade de Engenharia da Universidade do Porto

§Computer Science Department, University of Rome, "La Sapienza", Italy

{iokazdarid,posymeon}@uth.gr,sk@gridnet.gr,{pdias,pedro,bloureiro}@lsts.pt,{gjanci,petrioli}@di.uniroma1.it

ABSTRACT

The energy restricted nature of underwater sensor networks directly affects the expected lifetime of autonomous deployments and limits the capabilities for long term underwater monitoring. Towards the goal of developing energy-efficient protocols and algorithms, researchers and equipment vendors require in-depth understanding of the power consumption characteristics of underwater hardware when deployed in-field. In this work, we introduce the EVERUN power monitoring framework, consisting of hardware and software components that were integrated with real equipment of the SUNRISE testbed facilities. Through the execution of a wide set of experiments under realistic conditions, we highlighted the limitations of model-based energy evaluation tools and characterized the energy efficiency performance of key protocols and mechanisms. The accuracy of the collected power data, along with the interesting derived findings, verified the applicability of our approach in evaluating the energy efficiency performance of proposed solutions.

KEYWORDS

Underwater Networking, Testbed Experimentation, Power Consumption Monitoring, Energy Efficiency

1 INTRODUCTION

Underwater Networking is a rapidly evolving research thrust, enabling the exploitation and monitoring of the vast natural resources existing in the undersea environment that covers more than 70% of the earth's surface. The key communication technology that enables these applications in the extreme underwater environment, is based on the propagation of Wireless Acoustic Signals. The recent advances in acoustic modem and sensor technologies have motivated the deployment of an increasing number of underwater sensors. Parallel to these technological advances, research has moved into the area of networking, resulting in the deployment of realistic experimentation platforms.

In this context, SUNRISE [8] is the first project offering open experimentation facilities, integrating physical systems with software development into the *"Internet of Underwater Things"*. SUNRISE provides a wide set of different underwater hardware device types that enable experimentation in sea environments. The SUNSET framework [19], developed by SENSES Lab [7], provides all core functionalities for implementing underwater sensor network (UWSN) protocols over multiple layers, considering also various underwater hardware devices. Despite the recent advances in the field of realistic UWSN testbed evaluation, experimental assessment of proposed schemes in terms of energy efficiency still lags behind. Currently, evaluation of energy consumption is only supported in the Simulation framework of SUNSET, thus failing to address the complexity of real scenarios and to support the high level of heterogeneity that characterizes UWSN hardware.

In this work, we develop the EVERUN power monitoring framework and integrate it with the SUNRISE facilities and SUNSET framework, for enabling researchers and underwater equipment vendors to characterize the performance of proposed protocols from an energy efficient point of view. The key contributions of our work are listed below:

- the developed system was integrated with autonomous underwater vehicles (AUVs) and gateway (GW) devices developed by UPorto - LSTS [12], which feature a vast variety of sensing, communication and navigation components.
- novel applications and services were developed on top of SUNSET to support experimental in-field validation, as a fully automated procedure.
- a wide set of experiments were executed under realistic conditions to characterize the power behavior of key UWSN devices at the component level.
- the energy efficiency of important protocol parameters and mechanisms was characterized, resulting in interesting insights.
- specific experiments were conducted both in the testbed and simulated through SUNSET to highlight modeling inefficiencies
- accurate collected power data were integrated with the Simulation framework to improve the energy modeling accuracy.

WiNTECH'17, October 20, 2017, Snowbird, UT, USA

ACM ISBN 978-1-4503-5147-8/17/10…$15.00

https://doi.org/10.1145/3131473.3131486

Component	Type of Asset	Voltage	Max Cons.	Power Save	Sampl. Rate	Range	Resistor
Evologics S2CR Acoustic Modem 18/34	LAUV & GW	BAT	80 W	2.5 mW	30 kHz	32.000:1	0.02 Ω
WiFi - Ubiquiti Picostation M2	LAUV & GW	12 V	8 W	-	120 kHz	-	0.1 Ω
Huawei E156G 3G USB Dongle	GW	5 V	2.5 W	-	30 kHz	-	0.2 Ω
GSM & Iridium	LAUV	5 V	8 W	-	30 kHz	-	0.2 Ω
Motor & Servomechanisms	LAUV	BAT	145 W	50 mW	20 kHz	2.900:1	0.01 Ω
Embedded PC	LAUV	5 V	10 W	-	120 kHz	-	0.02 Ω

Table 1: Considered components and characteristics per device type

The rest of the paper is organized as follows. Section 2 lists important requirements and considerations for the development of online energy monitoring tools. Related work is discussed in Section 3, while system implementation and integration with SUNRISE appear in Sections 4 and 5 accordingly. Finally, Section 6 presents our detailed experimental evaluation and Section 7 concludes the paper. For simplicity, for the rest of the paper we refer to the selected assets, AUV and GW nodes, as the devices under test or DUT.

2 KEY REQUIREMENTS

In this section, we list the key requirements for enabling online power metering in UWSN testbeds, along with the implementation options that we pursued.

Noninvasive operation: Energy monitoring procedure should not interfere with the normal operation or affect the actual energy consumption of the DUT. This suggests that the monitoring device should be powered from an independent power source, or alternatively the point of measurement should be confined to the component of the DUT to be measured. Moreover, it implies that the monitoring device should not rely on DUT resources for computation tasks, but instead perform the monitoring procedure in an autonomous fashion, so that the consumption of the DUT remain unaffected. In our setup, the point of measurement is properly placed on each module of the DUT and the developed device features an embedded system for the required assignments.

Online monitoring: Online monitoring needs to be applied, to enable energy efficiency evaluation under composite configurations and topologies. The proposed framework allows power monitoring in parallel with the execution of real UWSN experiments.

Adaptation to different device types: DUT feature various components that exhibit unique energy consumption profiles, implying that individual components should be independently monitored. Due to this fact, the developed monitoring device follows a rather generic measurement procedure applicable to any type of device, also featuring several individual input channels to enable parallel monitoring of multiple components.

Dynamic range: The components of the DUT may exhibit a perplex array of energy profiles, depending on the application scenario. The energy monitoring system must feature a wide dynamic range spanning the entire spectrum of possible current draws. The proposed device features high resolution ensuring sufficient capturing of dynamic transitions.

High sampling rate: To adequately monitor the consumption of the DUT, even the shortest in duration events of each discrete component should be considered to determine the proper sampling rate. The developed device features a high sampling rate unit to enable precise monitoring of all possible events, over several input channels, which last only a few μs.

Long-term monitoring: DUT are designed to execute missions lasting several hours. To this end, the proposed system should feature sufficient capabilities in terms of monitoring duration. Considering the expected duration along with the defined sampling rate and resolution, we equipped our system with enough storage space to locally cache the acquired measurements, prior to the offloading.

Small-size & low-cost hardware: A small-sized device eases the installation phase, requiring the least possible space for placement, while low-cost hardware allows large-scale deployments. Our monitor is a credit-card sized device, comprised of low-cost components.

3 RELATED WORK

In this section we discuss the relevant works in the fields of in-situ power meters and UWSN simulation frameworks.

In the first domain, we distinguish the following works as state-of-the-art. SPOT [14] power meter, tailored to WSN platforms, provides a wide-dynamic range of 45.000:1 and resolution lower than 1 μA. However, it monitors the energy consumption over a predefined period, rather than obtaining fine-detailed power measurements. iCount [13] uses an alternative principle for power monitoring, in which energy data inferred from the frequency of the pulse that appears on the inductor pin of the switching regulator that is used to power the DUT. This method enables power consumption monitoring that requires no extra hardware than that of measuring the pulse frequency, but it suffers from high error rates that can reach up to 20% and provides low measurement resolution. Another in-situ power meter is Nemo [21], which is a high fidelity tool that employs an array of resistors that are dynamically switched towards adjusting the shunt resistance depending on the current load in order to obtain better results. To this end, it supports a dynamic range of 250.000:1, while attaining very low measurement error. All the aforementioned solutions focus on WSN applications and rely on the host node to cache, compute and propagate the collected results, which rather affects the consumption of the DUT and reduces the attained accuracy. Moreover, all stated works do not support parallel monitoring of different components of the DUT. Finally, our previous works [15, 16] support on-line power consumption monitoring of testbed infrastructure, featuring long-term capabilities. However, it has limited sampling-rate and resolution, while it does not support monitoring of different components in parallel.

In the field of energy efficiency characterization of UWSN protocols, currently only the DESERT [18] and SUNSET [19] simulation frameworks support power modeling of relevant equipment. Both frameworks extend the open source NS2 simulation engine to support various underwater hardware devices and monitor energy consumption at the device level, when running in Simulation mode. Between the two, SUNSET provides a more accurate energy model

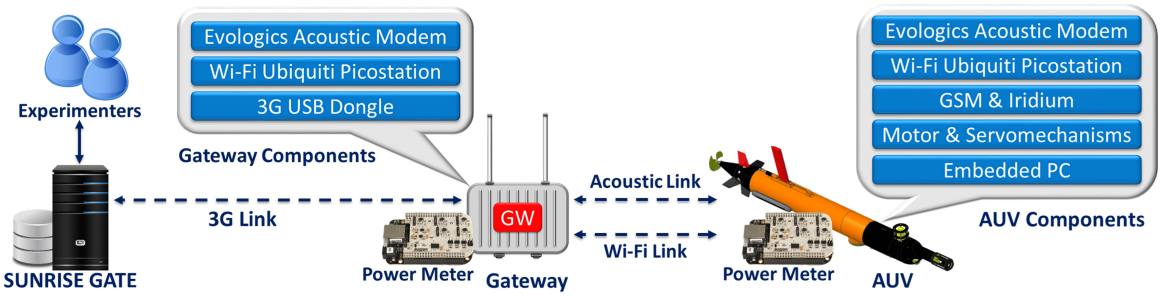

Figure 1: EVERUN power consumption monitoring framework, integrated with SUNRISE testbed

that also supports the configuration of different transmission levels for the acoustic hardware, while not currently supporting modeling of energy consumption behavior for AUV devices. Nonetheless, both frameworks do not offer support for energy efficiency evaluation during realistic sea experimentation.

4 FRAMEWORK CONSIDERATIONS

In this section we present the UPorto - LSTS experimental facility, investigating the specifications of the assets under consideration.

4.1 UPorto - LSTS testbed

The UPorto - LSTS testbed [17] is targeted at supporting collaborative evaluation and testing of network behavior and control of surface and underwater vehicles. The testbed is remotely accessible, enabling experimenters to evaluate their algorithms and protocols, and supports operations such as environmental monitoring and seabed mapping. It is deployed in the Leixoes marina located 5km south of Porto harbour, in Portugal.

The key components of the testbed are, the Light Autonomous Underwater Vehicles (LAUVs) and the Manta gateway. The first is a torpedo shaped vehicle with one propeller and 4 control fins. Its maximum speed is 2m/s, while it can reach up to 100m depth. The LAUVs integrate a wide set of sensors and systems to deliver the supported functionalities in UWSN experimentation, such as sidescan/imaging sonars, environmental sensors, video cameras, and several other modules. Moreover, they are equipped with a vast number of network devices, like acoustic modems, WiFi, GSM and Iridium interfaces. The second component is the Manta gateway, which is a portable communication hub, supporting several types of wireless and acoustic networks, aiming at providing backbone network to the LAUVs.

4.2 Specific Requirements & Considerations

In our work, we identified a specific subset of components that exhibit varying consumption patterns affected by the executed mission's characteristics, and remarkably affect the duration of UWSN missions. Namely, we consider the power hungry LAUV motor and acoustic hardware, along with the wireless networking interfaces and the embedded PC. In Table 1, we present the list of considered components per device type. Notably, there are some components that are coupled together in the same power rail, thus we can only measure the aggregated power consumption. More specifically, those components are the LAUV motor along with the servomechanisms that actuate the fins and the GSM interface that is integrated in the same board with the Iridium module.

Each LAUV is equipped with a 7S Li-ion 25.9 V battery pack, while the GW features a similar pack with lower capacity. As shown in Table 1, some of the components are powered by the regulated rails of 5 V and 12 V, while some others directly by the batteries. To this end, for the LAUVs, we require 5 channels for monitoring the current draw of the selected components and 3 additional inputs to monitor the voltage rails, in order to ensure accurate power results. Notably, it is vital to monitor the voltage rails, especially of the battery powered components, since it presents high variations depending on the load and the remaining charge.

To properly determine the required sampling rate for each component we should identify the shortest possible events in terms of duration that actually affect its power consumption and estimate their length. In the case of the WiFi interface it is the propagation of a small size packet at the highest Physical Transmission Rate (TX_R). For the under consideration WiFi device the maximum supported TX_R is 150 Mbps, when using the MCS7 modulation & coding scheme, while employing a 40 MHz Bandwidth channel. Moreover, the shortest feasible packet is of 300 Bytes, which implies that the time required for its transmission is 16 μs. Thus, we decided to sample the WiFi module at 120 KHz, which is twice the required rate for capturing such events. Concerning the CPU, which varies based on the running process, it is particularly important in special scenarios involving local processing of measurements at the host PC, we decided to use the same high speed sampling, to ensure accurate monitoring. As for the acoustic hardware [4] the shortest event is the propagation of the preamble signal which requires a sampling rate of 30 kHz. Similarly, GSM and Iridium modules require a sampling rate of 30 kHz and the motor along with the servomechanisms a rate of 20 kHz. Notably, we performed extensive measurements with the maximum supported sampling rate in order to derive safe results. Table 1 summarizes the extracted sampling rates.

To determine the required resolution we consider the components that feature power saving mode that typically exhibit wide range in their consumption pattern. As shown in Table 1 only acoustic modems and motors support power saving state. Acoustic modems may drain minimal power amounts of 2.5 mW when in idle state, while reaching up to 80 W when transmitting at the highest power configuration. This implies that their consumption range can reach up to 32.000:1, which is the highest range of the components under consideration. Finally, in order to achieve long-term monitoring we need to ensure adequate storage space, taking into consideration the sampling rate and the resolution.

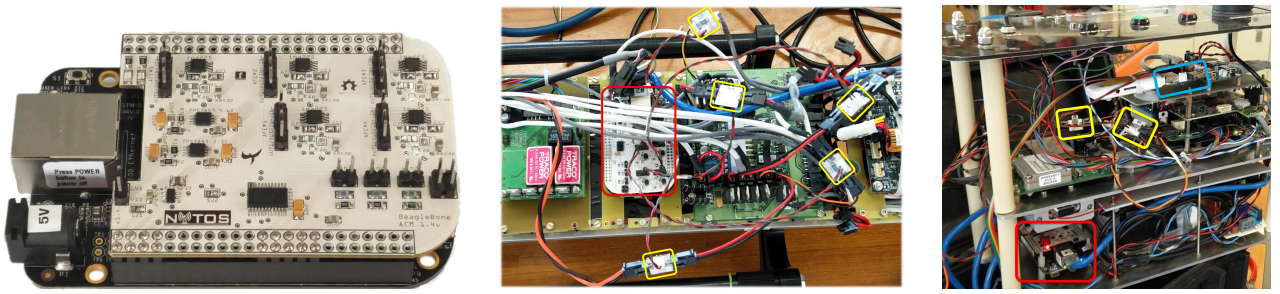

(a) Developed power monitoring device (b) LAUV vehicle installation (c) Manta gateway installation

Figure 2: Developed monitoring device & Integration with SUNRISE assets

5 SYSTEM IMPLEMENTATION & INTEGRATION

In this section, we present the architecture of the EVERUN framework and the development of the monitoring device along with our implementation choices. Lastly, we present the integration steps towards the implementation of a functional monitoring system.

5.1 Energy Consumption Monitoring Framework Architecture

The architecture illustrated in Fig. 1 comprises of three tiers: the sensing, the intermediate that relays messages from the DUT to the outside world and the user framework. The first tier consists of the power metering device deployed inside the DUT (Fig. 2(b)) and properly connected to measure the components under consideration. The device is connected to the LAN network of the DUT through its Ethernet port, taking advantage of the existing Ethernet switch that is used to support the connection of several on-board devices. In addition, the monitoring device hosts a web-service that integrates a set of commands using a RESTful API to remotely configure its parameters and control the activation/operation of the monitoring procedure.

The second layer is responsible for relaying messages between the user framework and the monitoring devices. To this end, we engaged the embedded PC of the DUT to issue the appropriate HTTP commands, for controlling the monitoring process and allowing the offloading of measurements. When a mission is performed by the LAUVs, the monitoring device is automatically instructed by the host CPU of the DUT to initiate the sampling procedure of the requested components at the specified sampling rate. When the mission has been completed, the DUT commands the monitoring device to halt the sampling operation. In turn, the acquired measurements are stored locally on the on-board storage, ready to be offloaded after the completion of each experiment with the aid of the SCP protocol.

Finally, the third entity is the user interface through which users access the testbed resources as well as design and execute their experiments. In our case, this is the SUNRISE GATE [20], which is a complete tool enabling users to specify the experiment parameters and configure the energy monitoring process. Through the SUNRISE GATE the user can load a completed experiment and replay the missions by using a simple web interface. Upon the completion of the experiment, the data retrieved from the device, processed and uploaded to the SUNRISE GATE server and the user is provided with the energy consumption data that correspond to the assets involved and components selected. When the user replays a mission the energy data illustrated in the form of a live line chart that is populated as the mission progresses.

5.2 Power Monitoring Device Development

The principle followed to measure the power consumption is the placement of a precise, low-impedance shunt resistor, in series with the component to be measured. The voltage drop across this resistor is proportional to the current drain, according to Ohm's law, enabling the extraction of power data. More details can be found in our previous work [15].

Embedded PC: The monitoring device is composed of different hardware and electronic components, constituting a unified solution able to address the requirements specified in Section 2. The core module is the BeagleBone Black Rev. C [1], which is a low-cost, embedded platform characterized by sufficient processing power capabilities (1GHz with 512MB RAM), low-power consumption and several communication interfaces. BeagleBone also supports several operating systems; in our prototype we used the Linux-based Debian OS [3] optimized for the BeagleBone hardware. All of the electronic components used for the power consumption sampling are hosted on a custom-made printed circuit board (PCB) daughterboard mounted on top of the embedded host device, as illustrated in Fig. 2(a). The embedded platform is responsible for controlling the peripheral units and implements the software architecture for the energy monitoring system. Furthermore, the device features an external microSD, used to locally cache the acquired measurements, prior to the offloading process. The BeagleBone along with the on-board electronics is of small size enabling ease of installation and inducing the overall low cost of ~80€.

Analog to Digital Converter: To convert the analog signal to digital we employed the Texas Instruments (TI) ADS8332 ADC IC [9]. The selected ADC features 8 input pins connected to its internal multiplexer that enables switching among the available signals in order to allow for parallel sampling of multiple components. Moreover, it features 16-bits resolution and high SNR of 91 dB, while performing conversions at 500 kSamples per second (kSps). The overall sampling rate is split among the configured channels. It supports 8 discrete channels, 5 for current and 3 for voltage measurements. Moreover, it achieves twice the maximum required range (64.000:1), while also exceeding the required aggregated sampling rate. We opted for the ADS8332, because it complies

with our defined requirements described in section 4 and clearly outperforms the BealgeBone's embedded ADC unit. Finally, given the specified sampling rate and speed and taking into consideration that a typical mission lasts up to 7 hours we calculated that our device will generate roughly 16 GByte of data in case of continuous monitoring. Thus, we attached a 32 GByte memory card to ensure long-term monitoring capabilities.

Analog Front-End: The analog front-end is a circuit that scales the observed voltage drop across the shunt resistor to a full-scale analog signal to ensure optimum signal-to-noise ratio (SNR) and enhances the accuracy of the sampled data. Notably, the observed voltage drop signal varies from a few mVolts to a hundred mVolts, while typical ADCs are sampling signals of a few Volts. Thus, it is imperative to use an amplification circuit, to deliver the required signal scale. In our implementation, we decided to utilize the TI INA225 [10] current-sense amplifier, which is based on a low-offset, zero-drift architecture supporting wide Bandwidth range of 250 kHz, thus making it ideal for our system and the defined requirements.

Supply & Reference Voltage: In our application we power the electronics by LAUV's 5V power rail that is used to power several on-board modules, hence it presents high variations in the voltage and features high-noise, induced by high-frequency components. The employed ADC & analog front-end ICs are highly sensitive, thus we integrated two TI TPS7A49 [11] ultra-low noise, high PSRR (Power Supply Rejection Ratio), regulators. One for powering the ADC IC and another one for the Analog Front-ends. This ensures a clean voltage rail and noise filtering. Moreover, the ADC converter requires a highly precise voltage reference, in order to accurately perform the conversion to a digital value. To this end, we employed the TI REF3233 [6] IC that delivers highly constant output, irrespective of the load on the device, power supply variations and temperature changes.

Custom SPI Implementation: The communication of the ADC IC with the host embedded device is realized through the SPI protocol. The native SPI interface speed on embedded devices, such as the Beaglebone board, imposes certain limitations in terms of the maximum throughput and the jitter between measurements. Notably, when using the native SPI interface we achieve sampling rates of up to a few kSps, thus bottlenecking the ADC. To this end, we utilized a special entity integrated in the processor of the Beaglebone, called PRU (Programmable Real-time Unit) [2, 5]. A PRU is a fast (200MHz, 32-bit) processor, programmed in ARM Assembly, ideal for applications that require high speed and precision. We implemented the SPI protocol on the PRU enabling fast (500 kSps), jitter-free and continuous communication between the embedded device and the ADC IC.

5.3 Power Monitoring Device Installation

In order to proceed with the integration, we placed individual shunt resistors per considered component, as shown in yellow color in Fig. 2(b) and 2(c) in both LAUVs and the Manta gateway. Notably, the power meter is highlighted with the red frame, the shunt resistors with the yellow and a USB extension board with an on-board shunt resistor to measure 3G Dongle's power with the blue one. The power monitoring device is connected with each resistor to monitor the differential signal. Moreover, the device is connected with the three different voltage rails to acquire voltage measurements. In order to select appropriate resistor value per component, we conducted a thorough in-lab investigation of the energy profile under high loads, to determine the maximum achievable drain per device component. Based on the above and considering the maximum supported input voltage of the INA225 monitor in our setup (132 mV), we calculated the appropriate resistance value, as shown in Table 1. To note that the installation is as less invasive as possible, while the application of the framework does not interfere with the operation of the assets.

Configuration	Level	Power Cons.
TX SPL	Max	25.95 W
TX SPL	Max -6 dB	9.34 W
TX SPL	Max -12 dB	4.34 W
TX SPL	Max -20 dB	2.76 W
RX Gain	Max	2.26 W
RX Gain	Max -20 dB	1.98 W

Table 2: Power consumption of Evologics S2CR 18/34 modem under various SPL and Gain configurations

6 EXPERIMENTS

Extensive UWSN experiments were conducted within the Leixões marina located in Porto, Portugal with the support of the UPorto - LSTS team. The employed devices include two Noptilus LAUVs and one Manta GW, which are all equipped with the developed power monitoring equipment. In the following experiments, we highlight how the consumption of each different device component varies when executing a real UWSN mission in the water.

6.1 Acoustic modems

6.1.1 Static channel conditions

In this first set of experiments, we focus on highlighting the device settings able to significantly impact the power consumption of acoustic hardware. For this purpose, we setup an acoustic link between two Evologics S2CR 18/34 modems under static channel conditions and simultaneously measure power consumption at both the transmitter and receiver side. Having experimented under various configurable parameters on Evologics equipment, we identified that the two core settings able to impact consumption are the Source Level affecting the sound pressure level (SPL) during transmission and the Gain Level that adjusts the input amplifier gain during reception. To experiment with these two parameters, we transmit saturated traffic between the two modems under the fixed PHY rate of 976 bps, by employing the "Send Instant Message" mode of operation. Under this setup, we vary the SPL and Gain configurations among the supported levels for both link sides and we illustrate the collected power measurements in Table 2.

Apart from considering the acoustic hardware settings directly impacting power drain, we also focus on parameters affecting overall energy consumption. As energy consumption is directly related to the duration of the frame exchange, we focus on the two key related parameters, namely the employed transmission PHY rate and the total length of exchanged frames. Evologics modems implement dynamic PHY rate adaptation through proprietary algorithms by default and do not offer configuration of PHY rates on demand, apart from the option to employ the "Send Instant Message" mode. In an effort to investigate the impact of frame exchange duration on energy consumption, we use the aforementioned setup to vary

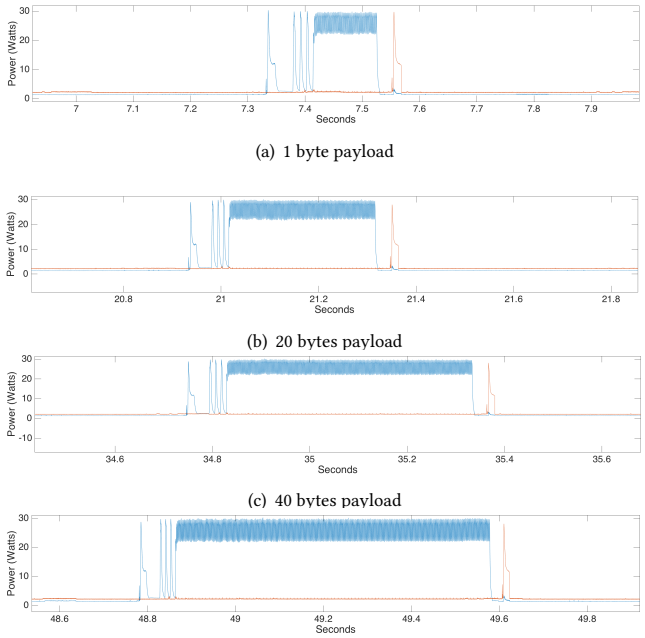

(a) 1 byte payload

(b) 20 bytes payload

(c) 40 bytes payload

(d) 64 bytes payload

Figure 3: Power consumption of Evologics S2CR 18/34 modem under various frame length transmissions

Payload (bytes)	TX Energy (J)	RX Energy (J)	TX Energy eff. (mJ/bit)	RX Energy eff. (mJ/bit)
1	3.56	0.44	445.4	15.4
20	8.50	0.85	53.17	12.6
40	13.78	1.32	43.08	11.93
64	19.29	1.78	40.19	11.57

Table 3: Energy consumption across varying payloads

the length of injected frames, up to the maximum supported length of 64 bytes.

In Fig. 3, we plot the instantaneous power consumption of the two modems under 4 indicative payload sizes of 1, 20, 40 and 64 bytes, where the blue and red lines illustrate the power consumption at the TX and RX side respectively. We clearly observe that each transmission consists of a fixed first part related with the frame preamble lasting approximately 75 ms and a second part that carries the actual data, whose duration depends on the payload length. In Table 3, we characterize the amount of energy that is consumed at each side, in terms of total consumed energy (J) and Energy efficiency (mJ/bit). The presented results quantify the improved energy efficiency (91% between the 64 and 1 byte cases for the TX part) that higher payload transmissions are able to offer, by amortizing protocol overheads, such as frame preamble, headers, etc. Our analysis can be further applied to study the energy impact of vendor specific techniques, such as frame aggregation, forward error correction and data compression.

6.1.2 Varying channel conditions

The second set of experiments on acoustic hardware focuses on highlighting the energy efficiency performance of different protocol configurations under varying channel conditions. For this purpose,

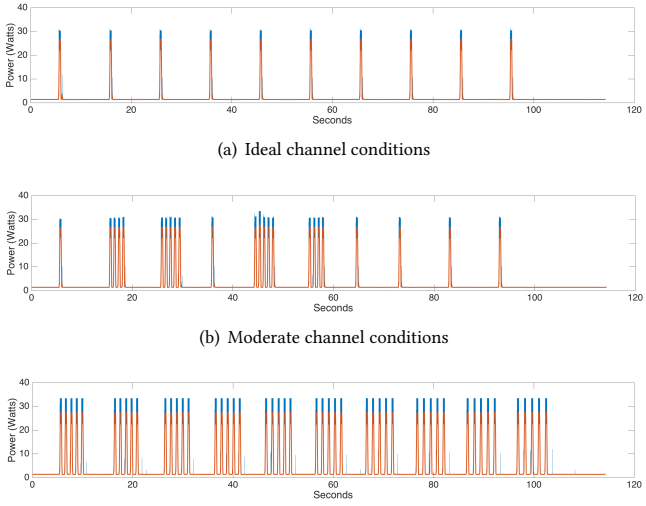

(a) Ideal channel conditions

(b) Moderate channel conditions

(c) Lossy channel conditions

Figure 4: Power consumption of Evologics S2CR18/34 modem under various channel conditions

we design an appropriate experimental scenario that relates the impact of retransmission attempts with energy consumption. Evologics modems support the configuration of the maximum number of retransmissions the device will perform to deliver an instant message after a failure. We exploit this feature and fix the number of maximum retries to 4, to experiment in a scenario including the transmission of 10 instant messages carrying a payload of 20 bytes at an interval of 10 seconds, while setting the maximum SPL-Gain settings. We repeat the experiment under three types of channel conditions, namely ideal (no retries), intermediate and lossy (max retries attempted per frame), by varying the distance between the acoustic modems.

In Fig. 4, we plot the instantaneous power consumption of the transmitting modem, across the three different scenarios. Considering that the maximum number of retries is fixed to 4, we observe that the number of attempted transmissions varies between 10 and 50, depending on the channel conditions. Focusing on the moderate channel conditions scenario, we see that a total number of 24 transmissions were attempted. In terms of energy consumption, the developed framework reported the values of 245.05 J, 364.06 J and 595.94 J, under ideal, moderate and lossy channel conditions accordingly. Given the fact that the Evologics software does not report the actual number of performed retries per failed delivery, we understand the inability to build an accurate energy evaluation tool, even when fed with highly accurate power values per device state, as the ones reported in Table 2. The inefficiency of such a static power model would induce modeling error of 48.5 %, when considering the ideal channel model instead of the moderate one. This finding highlights the disadvantage of modeling approaches followed by simulator and emulation based systems in deriving the power consumption under realistic experimentation conditions. Through the EVERUN, we are able to capture events related to specific protocol implementations, such as retransmission policies, transmission power adaptation, etc. and quantify their energy impact towards aiding in the development of energy efficient protocols.

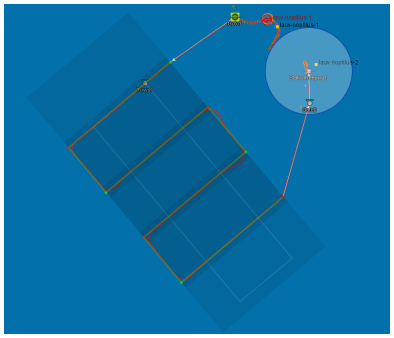

Figure 5: LAUV route

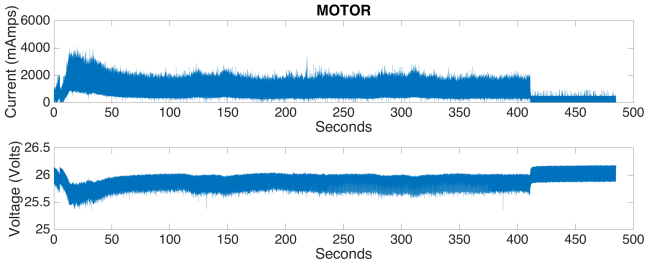

Figure 6: LAUV motor power consumption

6.2 LAUVs

6.2.1 Real experiments

We start our experimentation with the Noptilus LAUVs, by investigating the vehicle parameters remarkably affecting power consumption. To this aim, we use different components, such as the motor, servos, under various settings e.g. depth or water current and evaluate the resulting power impact. Through this investigation, we identified that the key setting able to affect consumption is the motor RPM (revolutions per minute), while the other parameters can only pose minimal impact. We characterize the impact of motor RPM, by executing an experiment with the Noptilus-1 LAUV, configured to move at the surface level when no water current is evident and vary the motor RPM across the values of 600 and 1300 that enable the device to start moving and 0 RPM to measure idle power consumption. Table 4 plots the collected power data, showing the wide range of power drain across different RPM settings. The power data appear to far exceed the results collected under identical RPM settings when applied in the lab with the LAUV not being in contact with water and the drift it results in.

We proceed with our second LAUV experiment, by instructing the Noptilus-1 LAUV to use the fixed speed of 1m/s, while following the specific route illustrated in Fig. 5 and consisting of 4 individual maneuvers. In the experimental logs, we observe that the mission is completed in 485 seconds and that the motor's RPM varies between 800 and 1100 in an effort to maintain the desired speed. Having processed the collected power data through the developed Matlab script, we generate the plot presented in Fig. 6 and clearly observe that the monitoring duration matches the experiment duration, verifying the achieved time synchronization exactly.

Focusing on the voltage subplot of Fig. 6, we observe high variation between 25.4 V and 26.2 V (voltage difference of 0.6 V), as a consequence of the voltage drop occurring across the resistance between the power supply and the monitored component. This finding highlights the importance of monitoring the voltage rail in parallel with the current draw, in order to increase the overall power monitoring accuracy. Considering a fixed voltage of 26.2 V, we would estimate the max instantaneous consumption of ~104.8 W instead of 101.6 W inducing a measurement error of ~3.15%.

Upon observation of the power subplot, we understand that the LAUV is moving for approximately 411 seconds, while it remains idle for the rest 74 seconds, as it has already reached its final way-point. The red line is used to point out the average power value calculated as a moving over a window of 1000 samples. During the moving phase, we see that the LAUV motor power consumption is quite stable apart from the initial phase, where higher power drain is observed during the speed increase until the target speed of 1m/s is achieved.

Motor RPM	Power (Watts)
0	3.05
600	14.52
800	23.39
900	30.36
1000	38.12
1100	46.94
1200	59.54
1300	71.12

Table 4: LAUV motor power consumption across RPM levels

Phase	Real dur. (sec)	Simulated dur. (sec)	Power (W)
Initial	0-50	0-50	44.69
Constant	50-411	50-378	23.89
Idle	411-485	378-485	1.95

Table 5: Power consumption measurements of LAUV motor experiment per phase

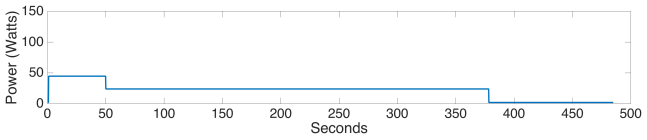

Figure 7: Simulated LAUV motor power consumption

6.2.2 SUNSET Simulated experiments

In an effort to compare the real power data, we proceed with the simulation of the last mission in the SUNSET simulator framework. SUNSET currently supports a simple mobility model for a generic LAUV. It allows to specify the way-points that the LAUV has to follow with the relative time in which the LAUV can stay fixed at each specific way-point (named in the following as station-keeping). Based on the LAUV's speed (specified in m/s) it is possible to track its position over time, given the restrictions of modeling movement as a linear line and not considering any other effect, such as current drifting. The real mission can be divided in three phases, as presented in Table 5 along with the individual duration and average power consumption, as derived through our calculations.

In an effort to increase the energy modeling accuracy of UWSN equipment in the SUNSET simulator, we incorporated a wide list of

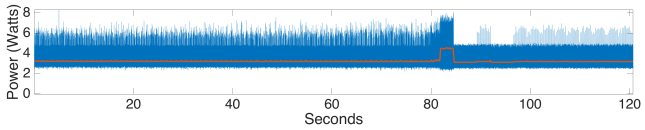

(a) WiFi interface

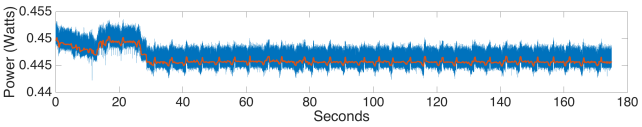

(b) 3G interface

Figure 8: Wireless communication interfaces

power data collected during real experiments (presented in Tables 2, 4), through the EVERUN framework. Moreover, we extended the simple energy model of SUNSET to consider the three individual states, namely the initial (starting from station-keeping), the constant during which the LAUV moves at a fixed speed and the idle while the LAUV remains in the station-keeping mode.

To demonstrate the extended energy model for the case of the LAUVs, we configured the in-field measurements presented in Table 5. The LAUV motor power consumption, as derived through SUNSET is presented in Fig. 7, clearly showing that the LAUV reaches its final destination 33 seconds earlier than the one in the real experiment. This is due to the simplified path followed in the simulation, which slightly differs from the real one followed by the Noptilus-1 LAUV (see Fig. 5). However, the overall simulated consumption for the total experiment duration is 10285 J, while the amount of the energy measured through the power monitor is 10789 J. This minor difference of ~4.9% verifies the ability of a simple energy model to estimate consumption quite accurately when fed with real measurements collected in-field.

6.3 Wireless communication interfaces

In this last set of experiments, we start by monitoring the exchange of data over WiFi, between the Manta GW and the Noptilus-2 LAUV. This type of communication is feasible only when the LAUV is moving at the surface level and is used to transfer protocol messages related to scheduled missions or to offload collected sensor measurements. The experimental logs show that the mission starts with the LAUV moving at the surface level up to approximately the 85th second, where the LAUV submerges and continues the mission underwater. In Fig. 8(a), we plot the power consumption of the WiFi interface. It is evident that frames are frequently exchanged until the LAUV submerges, while later WiFi activity decreases. The WiFi power consumption occurring while underwater is related to periodic transmissions of WiFi probe frames, in an effort to re-establish the WiFi link. We note that the consumption of the WiFi link ranges to a few Watts, since we refer to an entire WiFi embedded system and not to a NIC.

Next, we focus on the consumption of the 3G interface of the Manta GW, which is used to provide remote access to the LAUVs over the Internet. Fig. 8(b) illustrates the collected power measurements for the 3G interface, clearly showing intervals of varying consumption related to the varying amounts of traffic transmitted over 3G. Power monitoring of wireless interfaces can be employed to characterize the energy overhead that the offloading of collected data can pose on the overall energy consumption of underwater missions. Moreover, it can aid in developing mechanisms able to dynamically select the employed technology for data offloading, towards minimizing energy expenditure.

7 CONCLUSIONS

In this work, we introduced the EVERUN framework that enables researchers to characterize the performance of proposed UWSN protocols from an energy efficient point of view. The developed system was integrated with real LAUV and GW components of the SUNRISE testbed-site in Porto and the SUNSET experimentation framework. Through the execution of a wide set of remote experiments, under realistic conditions, we characterized the power behavior of key UWSN hardware and collected valuable insights about the energy efficiency of important protocol parameters and mechanisms. Inefficiencies of simulation-based energy evaluation tools were highlighted, while the delivered modeling accuracy was improved through the incorporation of accurate power data collected through EVERUN.

ACKNOWLEDGMENTS

The research leading to these results has received funding from the European Union's Seventh Framework Programme under grant agreement no. 611449 (SUNRISE Project).

REFERENCES

[1] *BeagleBone Black Rev. C Embedded board.* http://beagleboard.org/BLACK.
[2] *Beaglebone PRU-ICSS Resources.* http://beagleboard.org/pru.
[3] *Debian Operating System.* https://www.debian.org/intro/about.
[4] *Evologics S2CR 18/34 Underwater Acoustic Modem.* https://www.evologics.de/en/products/acoustics/s2cr-18-34.html.
[5] *Introduction to Beaglebone PRUs.* http://exploringbeaglebone.com/chapter13/.
[6] *REF3233 reference circuit.* http://www.ti.com/product/REF3233.
[7] *SENSES Lab.* http://senseslab.di.uniroma1.it/.
[8] *SUNRISE FP7 research project.* http://fp7-sunrise.eu.
[9] *TI ADS8332 Analog to Digital Converter.* http://www.ti.com/product/ads8332.
[10] *TI INA225 Current Monitor.* http://www.ti.com/product/ina225.
[11] *TPS7A49 ultra-low noise linear regulator.* http://www.ti.com/product/TPS7A49.
[12] *UPorto - LSTS (Underwater Systems and Technology Laboratory).* http://lsts.fe.up.pt.
[13] Prabal Dutta, Mark Feldmeier, Joseph Paradiso, and David Culler. Energy Metering for Free: Augmenting Switching Regulators for Real-Time Monitoring. In *Proc. of IPSN '08.*
[14] Xiaofan Jiang, Prabal Dutta, David Culler, and Ion Stoica. Micro Power Meter for Energy Monitoring of Wireless Sensor Networks at Scale. In *Proc. of IPSN '07.*
[15] Stratos Keranidis, Giannis Kazdaridis, Virgilios Passas, Thanasis Korakis, Iordanis Koutsopoulos, and Leandros Tassiulas. Online Energy Consumption Monitoring of Wireless Testbed Infrastructure Through the NITOS EMF Framework. In *Proc. of WiNTECH '13.*
[16] Stratos Keranidis, Giannis Kazdaridis, Virgilios Passas, Thanasis Korakis, Iordanis Koutsopoulos, and Leandros Tassiulas. 2014. NITOS Energy Monitoring Framework: Real Time Power Monitoring in Experimental Wireless Network Deployments. *SIGMOBILE Mob. Comput. Commun. Rev.* 18, 1 (Feb. 2014).
[17] R. Martins, J. B. de Sousa, R. Caldas, C. Petrioli, and J. Potter. SUNRISE project: Porto university testbed. In *Proc of UComms '14.*
[18] Riccardo Masiero, Saiful Azad, Federico Favaro, Matteo Petrani, Giovanni Toso, Federico Guerra, Paolo Casari, and Michele Zorzi. DESERT Underwater: An NS-Miracle-based framework to design, simulate, emulate and realize test-beds for underwater network protocols. In *Proc. of Italian Networking Workshop '13.*
[19] Chiara Petrioli, Roberto Petroccia, John R. Potter, and Daniele Spaccini. The SUNSET framework for simulation, emulation and at-sea testing of underwater wireless sensor networks. In *Proc. of Ad Hoc Networks '15.*
[20] C. Petrioli, R. Petroccia, D. Spaccini, A. Vitaletti, T. Arzilli, D. Lamanna, A. Galizial, and E. Renzi. The SUNRISE GATE: Accessing the SUNRISE federation of facilities to test solutions for the Internet of Underwater Things. In *Proc. of UComms '14.*
[21] Ruogu Zhou and Guoliang Xing. Nemo: A High-fidelity Noninvasive Power Meter System for Wireless Sensor Networks. In *Proc. of IPSN '13.*